European Community on Computational Methods in Applied Sciences

ECCOMAS Thematic Conference

COMPDYN 2021

8th International Conference on Computational Methods in Structural Dynamics and Earthquake Engineering

PROCEEDINGS

Volume I

M. Papadrakakis, M. Fragiadakis (Eds.)

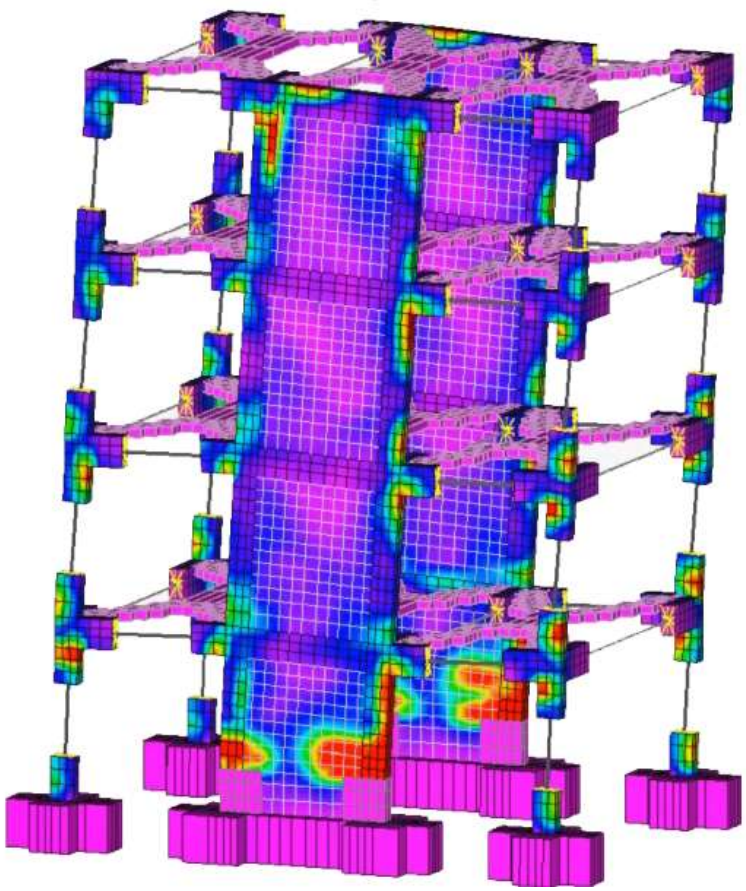

An IACM Special Interest Conference

COMPDYN 2021

Computational Methods in Structural Dynamics and Earthquake Engineering

Proceedings of the 8th International Conference on Computational
Methods in Structural Dynamics and Earthquake Engineering
Streamed from Athens, Greece
28-30 June 2021

Edited by:

M. Papadrakakis
National Technical University of Athens, Greece

M. Fragiadakis
National Technical University of Athens, Greece

A publication of:

Institute of Structural Analysis and Antiseismic Research
School of Civil Engineering
National Technical University of Athens (NTUA)
Greece

COMPDYN 2021
Computational Methods in Structural Dynamics and Earthquake Engineering
M. Papadrakakis, M. Fragiadakis (Eds.)

First Edition, September 2021

© The authors

ISBN (set): **978-618-85072-5-8**
ISBN (vol I): **978-618-85072-3-4**

PREFACE

This volume contains the full-length papers presented in the 8th International Conference on Computational Methods in Structural Dynamics and Earthquake Engineering (COMPDYN 2021) that was streamed from Athens, Greece on June 28-30, 2021.

COMPDYN 2021 is one of the 32 Thematic Conferences of the European Community on Computational Methods in Applied Sciences (ECCOMAS) which were held in 2021 and is also a Special Interest Conference of the International Association for Computational Mechanics (IACM). The purpose of this Conference series is to bring together the scientific communities of Computational Mechanics, Structural Dynamics and Earthquake Engineering, to act as a forum for exchanging ideas in topics of mutual interests and to enhance the links between research groups with complementary activities. We believe that the communities of Structural Dynamics and Earthquake Engineering will benefit from their exposure to advanced computational methods and software tools which can highly assist in tackling complex problems in dynamic and seismic analysis and design of structures, while also giving the opportunity to the Computational Mechanics community to be exposed to very important engineering problems of great social interest.

The COMPDYN 2021 Conference is supported by the National Technical University of Athens (NTUA), the European Association for Structural Dynamics (EASD), the European Association for Earthquake Engineering (EAEE), the Greek Association for Computational Mechanics (GRACM).

The editors of this volume would like to thank all authors for their contributions. Special thanks go to the colleagues who contributed to the organization of the Minisymposia and to the reviewers who, with their work, contributed to the scientific quality of this e-book.

M. Papadrakakis
National Technical University of Athens, Greece

M. Fragiadakis
National Technical University of Athens, Greece

ACKNOWLEDGEMENTS

The conference organizers acknowledge the support towards the organization of the "8th International Conference on Computational Methods in Structural Dynamics and Earthquake Engineering", to the following organizations:

- European Community on Computational Methods in Applied Sciences (ECCOMAS)
- International Association for Computational Mechanics (IACM)
- European Association for Structural Dynamics (EASD)
- European Association for Earthquake Engineering (EAEE)
- Greek Association for Computational Mechanics (GRACM)
- Hellenic Society for Earthquake Engineering (HSEE)
- School of Civil Engineering, National University of Athens (NTUA)

Plenary Speakers and Invited Session Organizers

We would also like to thank the Plenary and Semi-Plenary Speakers and the Minisymposia Organizers for their help in the setting up of a high standard Scientific Programme.

Plenary Speakers: Sondipon Adhikari, Peter Betsch, Hong Hao, Boris Jeremic, Geert Lombaert , Gabriele Milani , Shinobu Yoshimura

Semi-Plenary Speakers: Denis Duhamel, Fernando Fraternali, Muneo Hori, Alexander Idesman , Jean-Mathieu Mencik, Giuseppe Muscolino

MS Organizers: Christoph Adam, Hamid Ahmadi, Ada Amendola, Giulia Angelucci, António Arêde, Davide Arezzo, Nikolaos P. Bakas, Rui Carneiro Barros, Manuel Braz-César, Bruno Briseghella, Eleonora Bruschi, Bruno Calderoni, Guido Camata, Luca Caracoglia, Sandro Carbonari, Donatello Cardone, Claudia Casapulla, Serena Cattari, Nicola Cavalagli, Liborio Cavaleri, Dimitrios Chronopoulos, Francesco Clementi, Marco Gaetani d'Aragona, Mario D'Aniello, Dario De Domenico, Maria Teresa De Risi, Matt DeJong, Carlo Del Gaudio, Ciro Del Vecchio, Pedro Delgado, Mariano Di Domenico, Raffaele Di Laora, Marco Di Ludovico, Luigi Di Sarno, Fabio Di Trapani, Beatrice Faggiano, Marco Filippo Ferrotto, Amedeo Flora, Antonio Formisano, Michalis Fragiadakis, Fernando Fraternali, Fabio Freddi, André Furtado, Stefano Galassi, Emanuele Gandelli, Linda Giresini, José A. González, Chiara Iacovino, Alper Ilki, Maria Iovino, Konstantinos Katakalos, Jin-Gyun Kim, Radek Kolman, Daniele Losanno, George C. Manos, Giuseppe Carlo Marano, George Markou, Angelo Masi, Konstantinos G. Megalooikonomou, Gabriele Milani, Lucia Minnucci, Fabrizio Mollaioli, Michele Morici, Lukas Moschen, Jiří Náprstek, Vanni Nicoletti, Ehsan Noroozinejad, Roger Ohayon, K. C. Park, Carlo Pettorruso, Vagelis Plevris, Maria Polese, Virginio Quaglini, Giuseppe Quaranta, Laura Ragni, Gian Andera Rassati, Paolo Ricci, Hugo Rodrigues, Emmanouil Rovithis, Juan Chiachío Ruano, Manuel Chiachío Ruano, Antonio Sandoli, Fabrizio Scozzese, Salvatore Sessa, Anastasios Sextos, P. Benson Shing, Castorina Silva Vieira, Aram Soroushian, Enrico Spacone, James Swanson, Francesca Taddei, Kumar Tamma, Marco Tanganelli, Roberto Tartaglia, Anton Tkachuk, Savvas Triantafyllou, Grigorios Tsinidis, Yiannis Tsompanakis, Enrico Tubaldi, Filippo Ubertini, Nicolò Vaiana, Humberto Varum, Michalis Vassiliou, Ilaria Venanzi, Gerardo M. Verderame, Stefania Viti, Marco Vona

SUMMARY

VOLUME I

Minisymposia

[12] W. Xu, C. P. Pantelides, Strong-axis and weak-axis buckling and local bulging of buckling-restrained braces with prismatic core plates, *Engineering Structures 153*, 2017, 279–289.

[13] P. Gelfi, G. Metelli, Prova sperimentale di un elemento diagonale di controvento ad instabilità controllata, in: Proc., *XXI Congresso CTA: Costruire con l'acciaio*, Catania, Italy, [only in Italian], 2007, pp. 169–176.

[14] Eurocode 8: Design of structures for earthquake resistance-part 1: general rules, seismic actions and rules for buildings, *European Committee for Standardization*, Brussels, 2005.

[15] P. Fajfar, Capacity spectrum method based on inelastic demand spectra*, Earthquake Engineering & Structural Dynamics 28,* 1999, 979–993.

COMPDYN 2021
8th ECCOMAS Thematic Conference on
Computational Methods in Structural Dynamics and Earthquake Engineering
M. Papadrakakis, M. Fragiadakis (eds.)
Streamed from Athens, Greece, 28-30 June 2021

INFLUENCE OF THE EFFECTIVENESS FACTORS IN ASSESSING THE SHEAR CAPACITY OF RC BEAMS STRENGTHENED WITH FRP

Piero Colajanni, and Salvatore Pagnotta

Department of Engineering, University of Palermo
Viale delle Scienze, Ed. 8, 90128, Palermo, Italy
email: {piero.colajanni, salvatore.pagnotta}@unipa.it

Abstract

Shear failure of RC beams strengthened with composite textiles is often affected by the different failure modes characterizing the FRP reinforcement. The most relevant analytical models for evaluating the shear capacity of RC beams strengthened with FRP take into account these failure modes by introducing an effectiveness factor "R", which reduces the ultimate FRP tensile stress. Moreover, the interaction between stirrups and FRP reinforcement leads to a reduced efficiency of the transverse steel reinforcement due to the brittle failure of composite textile which hinders the yielding of all the stirrups involved by critical crack. In this regard, some analytical models introduce an effectiveness factor "r", aiming at reducing the yielding stress of stirrups. The procedures to calculate the above two parameters represent the main differences characterizing most of analytical models, significantly influencing their results. For this reason, the present paper focuses on the comparison of the different procedures to assess the effectiveness factors, proposing a new procedure for each effectiveness factor by modification of already existing formulations. Influence of the arrangement of composite reinforcement on the efficacy of stirrups, affected by brittle failure of FRP, is considered by means of the ratio between effective strain of composite to yielding strain of steel. The proposed procedures are employed in a design-oriented analytical model able to calculate the shear strength of RC beams retrofitted with FRP reinforcement arranged in any direction. The model is formulated aiming at representing an extension of EN1992 shear model to beams strengthened with FRP. The efficacy of the proposed procedures is assessed by comparing the experimental results against the predictions obtained via the design-oriented model and the above-mentioned analytical models.

Keywords: Instructions, ECCOMAS Thematic Conference, Structural Dynamics, Earthquake Engineering, Proceedings.

1 INTRODUCTION

Over the last years, several research groups have made significant efforts to develop innovative structures, able to significantly reduce structural damage caused by destructive earthquakes [1-6]. Nevertheless, due to different factors (e.g. costs, business disruption, design limitations), a considerable share of construction market is still devoted to retrofit existing RC structures, especially those built between 1950s and 1970s, whose seismic performances are unsatisfactory if compared to recently built structures. To this aim, among the different techniques used, externally bonded Fiber-Reinforced Polymer (EB-FRP) is one of the most employed, thanks to its excellent mechanical performance to density ratio.

During the last two decades, several mechanical models have been developed to assess flexural capacity and confinement effect of RC members retrofitted with externally wrapped composite reinforcement (e.g. [7, 8]). On the contrary, it is challenging to develop analytical models able to accurately account for all the resisting mechanisms influencing shear behavior of RC members (e.g. aggregate interlock, shear span to depth ratio, size effect, dowel effect, ductility demand), and the topic is still widely debated in the literature [9-11]. Some shear capacity models (such as [12, 13]) were developed on the basis of the strut-and-tie resisting scheme, by using an additive approach. However, these models assume that there is no interaction between shear contributions provided by concrete, steel stirrups and FRP reinforcement, and each contribution is achieved at shear failure. Nevertheless, experimental results showed that this interaction occurs, and may lead to both a reduced shear contribution provided by steel stirrups due to brittle failure of FRP which can be achieved before that all stirrups passing through shear critical crack yield, and a reduced shear contribution provided by FRP due to possible limitation of the ultimate strain [14-16].

Differently from the American codes, those developed in Europe (e.g. [17-20]) evaluate shear capacity of retrofitted RC members by means of truss mechanism with variable inclination of concrete strut, consistently with that used by [21] for ordinary RC members. However, uncertainty arises when assessing shear capacity provided by concrete strut, being no common solution in the selection of the angle of reinforcement to be used in the case of simultaneous presence of steel stirrups and FRP reinforcement arranged with different inclinations.

In this framework, the present paper focuses on the comparison of the different procedures to assess the effectiveness factors, proposing new procedures for the effectiveness factors dedicated to FRP and steel stirrups, by modification of already existing formulations. Influence of the arrangement of composite reinforcement on the efficacy of stirrups, affected by brittle failure of FRP, is considered by means of the ratio between effective strain of composite to yielding strain of steel. The proposed procedures are employed in a design-oriented analytical model able to calculate the shear strength of RC beams retrofitted with FRP reinforcement arranged in any direction. The model is formulated aiming at representing an extension of EN1992-1-1 shear model to beams strengthened with FRP. The main advantage of this model is the capability of simultaneously taking into account the presence, and their mutual influence, of steel stirrups, FRP reinforcement and concrete strut, in assessing shear capacity of retrofitted members. Closed-form equations are provided, for any amount and arrangement of shear reinforcement, able to calculate stress acting at failure on steel stirrups, FRP reinforcement and concrete strut, as well as angle of inclination of concrete stress field with respect to member axis. The accuracy of the proposed procedures is assessed by comparing the experimental results against the predictions obtained via the design-oriented model and the above-mentioned analytical models.

Moreover, a modified version of the model suggested by CNR is proposed and validated, aimed at overcoming the inaccuracy of the original model when assessing shear capacity of

concrete strut. In fact, in this case CNR model considers the angle of inclination of FRP reinforcement only, neglecting the presence of stirrups. The modified version of CNR, named CNRm, proposes to calculate an equivalent angle of shear reinforcement included in the evaluation of shear strength of concrete strut, obtained as a weighted average between shear capacity provided by steel stirrups and FRP reinforcement.

2 DESIGN-ORIENTED MODEL

Colajanni et al. [22] proposed a model based on the stress field approach, able to assess the shear capacity of RC members having transverse reinforcement arranged with two different inclinations. Here, that model is modified to be applied in the case of RC beams retrofitted with FRP reinforcement inclined in any direction. The proposed model also represents the extension of a model based on the stress field approach, able to assess shear strength of retrofitted RC beams with vertically-oriented FRP reinforcement only [23]. On the basis of the same assumption of the models proposed in [22, 24], shear capacity of a strengthened RC beam can be assessed by means of three different equations, obtained by calculating the vertical equilibrium of beam segments, identified via three different sections parallel to stress field directions of concrete strut, steel stirrups, and FRP reinforcement, respectively (Figure 1).

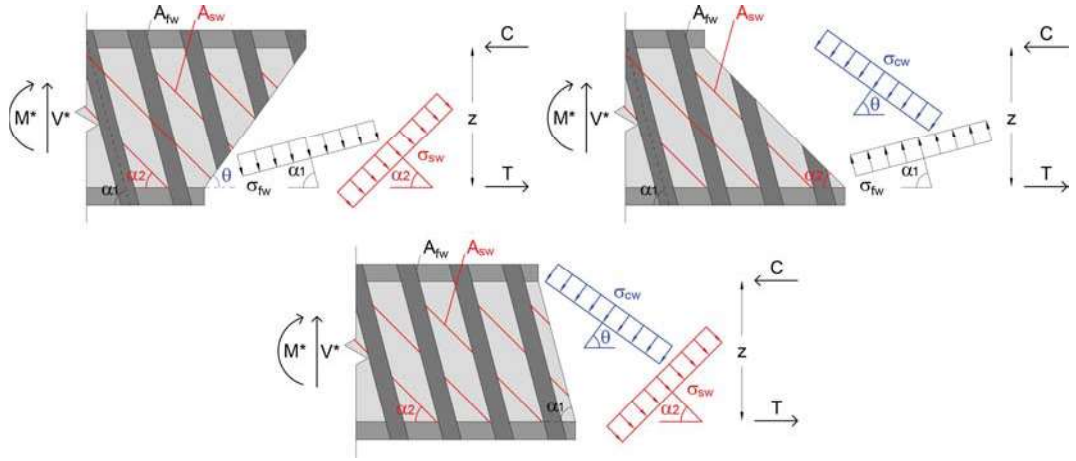

Figure 1: Different beam segments identified through three sections parallel to stress field direction of: concrete strut (a); steel stirrups (b); FRP reinforcement (c).

By doing so, each of the three equilibrium equations, which are given below, depends only on two stress fields, and can be easily solved:

$$v = R\tilde{\sigma}_{fw}\,\omega_{fw}\left(\cot\theta+\cot\alpha_1\right)\sin^2\alpha_1 + r\,\tilde{\sigma}_{sw}\,\omega_{sw}\left(\cot\theta+\cot\alpha_2\right)\sin^2\alpha_2 \tag{1}$$

$$v = \tilde{\sigma}_{cw}\left(\cot\theta+\cot\alpha_2\right)\sin^2\theta + R\,\tilde{\sigma}_{fw}\,\omega_{fw}\left(\cot\alpha_1-\cot\alpha_2\right)\sin^2\alpha_1 \tag{2}$$

$$v = \tilde{\sigma}_{cw}\left(\cot\theta+\cot\alpha_1\right)\sin^2\theta + r\,\tilde{\sigma}_{sw}\,\omega_{sw}\left(\cot\alpha_2-\cot\alpha_1\right)\sin^2\alpha_2 \tag{3}$$

In the above equations v is the shear strength made non-dimensional with respect to $b_w z f_{cm}^{'}$ (b_w section width), $\tilde{\sigma}_{fw}=\sigma_{fw}/f_{fu}$, $\tilde{\sigma}_{sw}=\sigma_{sw}/f_{syw}$, $\omega_{fw}=\left(2b_f t_f f_{fu}\right)/\left(b_w s_f \sin\alpha_1 f_{cm}^{'}\right)$, and $\omega_{sw}=\left(A_{sw}f_{syw}\right)/\left(b_w s_w \sin\alpha_2 f_{cm}^{'}\right)$ are the non-dimensional stresses and the mechanical ratios of FRP reinforcement and steel stirrups, respectively, f_{fu} is the nominal rupture stress of the fiber, R the strain and stress "effective" coefficient (effective strain $\varepsilon_{fe}=\varepsilon_{fu}\,R$, effective stress $f_{fe}=f_{fu}\,R=E_f\,\varepsilon_{fe}$), and r is the reduction factor

of the efficiency of the steel stirrups. The values of these efficiency coefficients will be investigated and assessed in the following sections.

The shear capacity of an RC beam is computed via the static theorem of theory of plasticity, which gives an assessment of the shear capacity as the maximum value among the possible solutions satisfying both the equilibrium condition (1)-(3) and the following inequalities of plastic admissibility:

$$0 \le \tilde{\sigma}_{cw},\ \tilde{\sigma}_{fw} \le 1 \qquad -1 \le \tilde{\sigma}_{sw} \le 1 \tag{4}$$

A plastic admissible condition is obtained by combining (1), (2) and (4), as follows:

$$0 \le \tilde{\sigma}_{cw} = \left(R\,\tilde{\sigma}_{fw}\,\omega_{fw} \sin^2 \alpha_1 + r\,\tilde{\sigma}_{sw}\omega_{sw} \sin^2 \alpha_2 \right)\left(1 + \cot^2 \theta\right) \le 1 \tag{5}$$

The above inequalities clarify the relation between the stress fields of the web concrete, steel stirrups and FRP reinforcement.

In this paper, only the case of major practical interest is considered, namely α_1 and $\alpha_2 \le 90°$. According to Colajanni et al. (2020), to evaluate the shear strength and $\cot\theta$ initially it is supposed that, at failure, the stress limit is reached simultaneously in the three stress fields (i.e. $\tilde{\sigma}_{cw} = \tilde{\sigma}_{fw} = \tilde{\sigma}_{sw} = 1$). Thus, on the basis of the upper limit imposed by Eq. (5), the first tentative value of the inclination of the web concrete stress field is obtained as follows:

$$\cot\theta = \sqrt{\left(R\,\omega_{fw} \sin^2 \alpha_1 + r\,\omega_{sw} \sin^2 \alpha_2 \right)^{-1} - 1} \tag{6}$$

Based on the results of the above equation, assuming $\cot\theta_{lim} = 2.5$, three cases are defined:

- $1 \le cot\theta \le 2.5$: the stress limit is reached simultaneously in the three stress fields, and shear resistance can be calculated by using Eq.(1) assuming $\tilde{\sigma}_{cw} = \tilde{\sigma}_{fw} = \tilde{\sigma}_{sw} = 1$;
- $cot\theta > 2.5$: the amount of FRP reinforcement and steel stirrups is not sufficient to induce attainment of the maximum resistance in the web concrete stress field. Thus, $cot\theta = 2.5$ is assumed, and the shear capacity is computed through Eq. (1), assuming $\tilde{\sigma}_{fw} = \tilde{\sigma}_{sw} = 1$. The stress value in the web concrete field can be calculated by using Eq. (5), in which $cot\theta = 2.5$;
- $cot\theta < 1$: shear failure is due to attainment of the stress limit in the web concrete stress field and in one of the two shear reinforcements. Therefore, the other shear reinforcement is in the elastic range at beam failure. Now it is assumed that $\alpha_1 < \alpha_2$. With the aim of determining if the maximum shear is given by Eq. (2) with the FRP reinforcement reaching the effective strain in tension ($\tilde{\sigma}_{fw} = 1$) or (unlikely event) by Eq. (3) with the steel stirrups yielding in compression ($\tilde{\sigma}_{sw} = -1$), the following inequality is employed:

$$R\,\omega_{fw} \sin^2 \alpha_1 \le 0.5 + r\,\omega_{sw} \sin^2 \alpha_2 \tag{7}$$

If the inequality is true, then the FRP reinforcement attains its stress limit, and the stress acting on the steel stirrups is computed as follows:

$$\tilde{\sigma}_{sw} = \left(0.5 - R\,\omega_{fw} \sin^2 \alpha_1\right) / \left(r\,\omega_{sw} \sin^2 \alpha_2\right) \tag{8}$$

Conversely, if the inequality is false, then the steel stirrups yield in compression, and the stress acting on the FRP reinforcement is calculated as follows:

$$\tilde{\sigma}_{fw} = \left(0.5 + r\,\omega_{sw} \sin^2 \alpha_2\right) / \left(R\,\omega_{fw} \sin^2 \alpha_1\right) \tag{9}$$

3 FRP EFFECTIVENESS FACTOR

Several experimental observations have shown that the failure of shear-strengthened RC beams with bonded FRP is often associated with achievement of a specific failure mode involving the textile material. The most common FRP failure modes reported in the literature [25, 26] are the following: failure of the FRP; debonding at the FRP-concrete interface; excessive width of the shear cracks and consequent loss of aggregate interlock; separation of the concrete cover along a vertical plane (peeling off) (e.g. [27]). To take these effects into account a reduced effective FRP design strength $f_{fe} = E_f \times \varepsilon_{fe}$, smaller than its nominal design strength $f_{fu} = E_f \times \varepsilon_{fu}$, was assumed. It was assessed by applying the effectiveness coefficient R to the nominal ultimate fiber strain. Over the last two decades, several formulations have been developed in order to estimate the above coefficient. In the proposed model, six different approaches to assessing the reduced effective FRP design strength are considered, with the aim of comparing their efficiency when introduced in the proposed model. Two of these six approaches are reported below, being assembled by using different equations reported in several papers, while the other four approaches are those suggested by ACI [12], CNR [17], fib [20], and Mofidi and Chaallal [30].

3.1 First approach: Khalifa and Nanni [28, 29] and Pellegrino and Modena [27]

According to the first approach, already used in [23], the value of R is the minimum among the three effectiveness coefficients R_i (i=1,2,3) proposed in [28, 29] and the fourth R_4 reported in [27], i.e. $R = min\{R_1, R_2, R_3, R_4\}$.

The equations selected to describe the four modes of failure are reported below. The efficiency coefficient R_1, which takes into account the tensile failure of the FRP, is computed by means of the following equation:

$$R_1 = 0.56\left(\rho_{fw} E_f\right)^2 - 1.22\left(\rho_{fw} E_f\right) + 0.78 \tag{10}$$

where E_f is the elastic modulus of the fibers. The coefficient R_2, representing the debonding phenomenon, is calculated using the following equation:

$$R_2 = \frac{\left(f_{ck}\right)^{\frac{2}{3}}\left(d_{ft} - \eta L_e\right)\left[738.93 - 4.06\left(E_f t_f\right)\right]}{\varepsilon_{fu} d_{ft} 10^6} \tag{11}$$

where L_e is the effective length, which is evaluated using the expression provided by ACI and CSA:

$$L_e = 23300 / \left(E_f t_f\right)^{0.58} \tag{12}$$

η is a parameter that takes into account the anchorage conditions, equal to 1 or 2 if the shear strengthening is U-shaped or side-only, respectively. The range of validity of Eq. (12) is $20 \le E_f t_f \le 90$. In case of complete wrapping or U-shaped strengthening with anchorages able to prevent a debonding effect, the coefficient R_2 is not taken into account. The coefficient R_3, limiting the shear crack width, is set equal to:

$$R_3 = 6 \cdot 10^{-3} / \varepsilon_{fu} \tag{13}$$

In the case of side-bonding and U-jacketing reinforcement, FRP failure often involves the separation of the concrete cover along a vertical plane (peeling off). Hence, the coefficient

proposed in [27] is assumed equal to:

$$R_4 = \frac{2 f_{ct} A_c \cos^2 \beta b_{c,v}}{n_f t_f L_f E_f \left[\left(h_f - L_e \right) / \left(h_f \right) \right] b_f \varepsilon_{fu}} \tag{14}$$

Further details about the parameters involved by Eq. (14) can be found in the above-mentioned paper.

3.2 Second approach: Chen and Teng [25, 26]

According to [25, 26] the coefficient of effectiveness is the minimum between two effectiveness coefficients, namely $R = \min\{R_5, R_6\}$. The effectiveness factor R_5 takes into account the tensile rupture of FRP, which usually occurs across the critical crack, correlating it with non-uniform strain distribution in the FRP along a shear crack. The authors, assuming proportionality of the fiber strain to the width of the shear crack, supposed an approximate strain linear distribution, where the FRP strain increases linearly from a minimum at the crack tip to a maximum at the lower end. Thus, R_5 can be expressed as:

$$R_5 = \frac{1 + (h_w - d_f)/z}{2} \tag{15}$$

where d_f = height of the FRP. Since experimental observations show that this kind of failure mode usually occurs in fully wrapped or U-wrapped RC beams, this coefficient must be considered only for these arrangements. Instead, the coefficient R_6 takes into account failure through debonding of FRP, which may occur when the bond length is not sufficient. According to [25] the stress in the FRP is variable along the bond length, and its maximum stress ($\sigma_{f,max}$) can be evaluated as:

$$\sigma_{f,\max} = 0.427 \beta_w \beta_L \sqrt{\frac{E_f \sqrt{f_c'}}{t_f}} \le E_f \varepsilon_{fu} \tag{16}$$

where β_w = coefficient of the FRP-to-concrete width ratio; β_L = bond length coefficient. These values can be calculated by using the following equations:

$$\beta_w = \sqrt{\frac{2 - w_f / s_f \sin\beta}{1 + w_f / s_f \sin\beta}} \tag{17}$$

$$\beta_L = \begin{cases} 1 & \text{if } \lambda \ge 1 \\ \sin\dfrac{\pi\lambda}{2} & \text{if } \lambda < 1 \end{cases} \tag{18}$$

where $\lambda = L_{max}/L_e$ = normalized maximum bond length; in which the maximum (L_{max}) and the effective bond length (L_e) are respectively:

$$L_{\max} = \begin{cases} \dfrac{h_{frp,e}}{\sin\beta} & \text{for U - wrap} \\ \dfrac{h_{frp,e}}{2\sin\beta} & \text{for side bonded} \end{cases} \tag{19}$$

$$L_e = \sqrt{E_f t_f / \sqrt{f_c'}} \tag{20}$$

where $h_{frp,e}$ is the effective height of the FRP (further details can be found in [25]). Thus, the effectiveness reduction factor R_6 can be expressed as:

$$R_6 = \frac{\sigma_{f,\max}}{E_f \varepsilon_{fu}} \begin{cases} \dfrac{2}{\pi\lambda} \dfrac{1-\cos\dfrac{\pi\lambda}{2}}{\sin\dfrac{\pi\lambda}{2}} & \text{for } \lambda < 1 \\ 1 - \dfrac{\pi - 2}{\pi\lambda} & \text{for } \lambda \geq 1 \end{cases} \tag{21}$$

4 STEEL STIRRUPS EFFECTIVENESS FACTOR

As recognized in several studies [14-16] the simultaneous presence of steel stirrups and FRP reinforcement leads to a reduction in the peak resistance provided by each shear reinforcement. The interaction between the two materials is expressed both in the decrease of the FRP shear contribution with the increase of the axial rigidity ratio between the internal steel and the external FRP [27] and in the inability of some or all of the steel stirrups, affected by critical fracture, to reach the yield strength due to FRP brittle rupture [14-16]. To overcome these drawbacks many models have been developed, connecting the interaction between the two reinforcement systems to their rigidities [30], or the shear crack width [31] or simply assuming a fixed reductive coefficient $\alpha = 0.75$ [15].

On the basis of the parameter proposed by [15], in this paper the r reduction parameter is defined by means of a bi-linear expression that relates the reduction of the contribution to the shear strength given by the steel reinforcement to the ratio between the component of FRP effective strain in the direction of the internal steel reinforcement $\varepsilon_{fe,sd}$ and the internal steel reinforcement yield strain ε_{syw}:

$$r = \begin{cases} 0.75 \dfrac{\varepsilon_{fe,sd}}{\varepsilon_{syw}} & \text{if } \varepsilon_{fe,sd} / \varepsilon_{syw} \leq 1.33 \\ 1 & \text{if } \varepsilon_{fe,sd} / \varepsilon_{syw} > 1.33 \end{cases} \tag{22}$$

where $\varepsilon_{fe,sd} = \varepsilon_{fe} \cos\varphi$ with φ equal to the angle between FRP reinforcement direction and steel stirrups. The reduction coefficient thus defined is able to take into account both that the strain of the most elongated steel stirrup, at beam failure, can be limited by the effective strain of the fiber, and that not all the stirrups along the critical crack are able to reach the yield strain. In particular, when $\varepsilon_{fe,sd}/\varepsilon_{sy} = 1$, only the most elongated stirrup, which intercepts the shear crack at the point of maximum width, can reach the yield strain (assuming perfect adhesion with concrete). It is also noted that r can take on a value less than 1 even if the ratio $\varepsilon_{fe,sd}/\varepsilon_{sy}$ is greater than 1. This makes it possible to take into account the second effect mentioned above, i.e. the non-uniform distribution of tension in the steel stirrups intercepted by the shear crack.

As will be seen in the following sections, the modulation of the reduction coefficient $\alpha = 0.75$ proposed in [15], through the ratio between the deformations of the interacting materials, makes it possible to minimize the inaccuracy of the proposed models due to overestimation of the steel resistance contribution.

The above effectiveness factor for steel stirrups is used in conjunction with effectiveness factors reported in sections 3.1 and 3.2 only. This is due to the fact that the effectiveness fac-

tor proposed by Mofidi and Chaallal [30] already considers reduction of contribution provided by steel stirrups, while models proposed by investigated codes do not suggest any effectiveness factor and are used in their original formulation.

5 MODIFIED VERSION OF CNR-DT 200 R1/2013 [17]

Shear capacity model suggested by CNR is developed with the purpose of representing a direct extension of the model proposed by EN1992-1-1 to evaluate shear capacity of ordinary RC members. Shear capacity of each element constituting the truss mechanism can be written in non-dimensional form, as well as shear capacity of retrofitted members, as given below:

$$\begin{aligned} v_s &= \omega_{sw}\left(\cot\theta+\cot\alpha\right)\sin^2\alpha \\ v_f &= \omega_{fw}\left(\cot\theta+\cot\beta\right)\sin^2\beta \\ v_c &= \left(\cot\theta+\cot\psi\right)/\left(1+\cot^2\theta\right) \\ v &= \min\left(v_s+v_f, v_c\right) \end{aligned} \tag{23}$$

In the third of (23), the angle α provided by CNR model is substituted with the to-be-determined angle ψ. In fact, considering the angle α would consequently neglect the presence, and its influence, of the other shear reinforcement when assessing shear strength of concrete strut. For this reason, a simple iterative procedure is proposed below to calculate angle ψ.

According to the suggestion of CNR code, in the original version of CNR model the angle ψ is set equal to angle β, while the inclination of concrete strut is assessed aiming at maximizing shear capacity of retrofitted RC member. Therefore, the sum of the first and second equation of (23) is equated to the third of (23), yielding:

$$\begin{aligned} &\cot^3\theta\left(\omega_{sw}\sin^2\alpha+\omega_{fw}\sin^2\beta\right)+\cot^2\theta\left(\omega_{sw}\sin^2\alpha\cot\alpha+\omega_{fw}\sin^2\beta\cot\beta\right)+ \\ &+\cot\theta\left(\omega_{sw}\sin^2\alpha+\omega_{fw}\sin^2\beta-1\right)=\cot\psi-\omega_{sw}\sin^2\alpha\cot\alpha-\omega_{fw}\sin^2\beta\cot\beta \end{aligned} \tag{24}$$

In the proposed version of CNR model, angle ψ contained in (24) is calculated by means of the following iterative procedure:

- A tentative $cot\theta$ value is assumed, based on the sum of the mechanical ratios of each shear reinforcement $\omega_{sw}+\omega_{fw}$ (alternatively a value of 1.75 can be used, being the average value of the range of variation of $cot\theta$ suggested by CNR);
- By means of the first and second equation of (23) are computed shear capacities v'_s and v'_f provided by steel stirrups and FRP reinforcement, respectively. These values are employed to calculate a weighted angle ψ' as $\psi' = (\alpha v'_s + \beta v'_f)/\left(v'_s + v'_f\right)$;
- The angle ψ' obtained is inserted in (24), yielding a new $cot\theta$ value.

This procedure can be used iteratively until the difference between two consecutive values of $cot\theta$ is negligible. However, numerical analysis performed by means of the above procedure showed that one iteration is sufficient to obtain accurate values of $cot\theta$.

6 DATABASE DESCRIPTION

With the aim of comparing the accuracy of the model described above, a database containing 158 specimens of RC beams having rectangular or T-shaped cross-sections, strengthened in shear by means of FRP strips or sheets was collected [14-16, 27, 32-51]. The specimen

characteristics and the test results are reported in in Table 1. The database contains beams strengthened with U-jacketing or complete wrapping schemes using carbon or glass fibers. The effective depth of the cross-section of the beams ranges between 155 and 831 mm, while the shear span is between 2.3 and 3.8. The transverse internal reinforcement is constituted by vertical steel stirrups whose maximum geometrical ratio is 0.48%. As regards FRP reinforcement, the ultimate tensile strength ranges between 106 and 4361 MPa, while the elastic modulus is comprised between 8 and 640 GPa. Lastly, the FRP geometrical ratio ranges between 0.04% and 3.00%.

The database was divided into two partial databases: DTB1, consisting of 138 specimens, in which the FRP reinforcement is arranged at right angles to the longitudinal axis of the member; DTB2, consisting of 20 specimens, in which the FRP reinforcement is arranged at an angle β different from 90°.

7 INFLUENCE OF EFFECTIVENESS FACTORS

The effectiveness factors described in previous sections are used to assess accuracy of the proposed design-oriented model, which is evaluated by means of the ratio between experimental shear capacity v_{exp} and theoretical prediction v_{the} of tests reported in Table 1. The parameters used to quantify the accuracy and reliability of the model are the average ratio between experimental and analytical values of shear capacity (Avg) and the Coefficient of Variation (CoV).

Generally speaking, all the approaches used to calculate effectiveness factor provide satisfactory results, as showed in Figure 2. Nevertheless, significant differences in the average and scatter values given by the analyzed approaches can be observed, highlighting the paramount influence of effectiveness factors in assessing shear capacity of RC beams. In fact, effectiveness factor suggested by ACI provides the best average value (0.99), while that of fib gives the worst one (0.83), overestimating significantly, in average, the shear capacity of beams. On the contrary, effectiveness factor provided by Mofidi & Chaallal leads to an overall underestimation of the shear capacity, with an average value of 1.12. With regard to effectiveness factors described in sections 3.1 and 3.2, and that suggested by CNR, they provide similar average values, showing an overall slight overestimation of shear capacity. Concerning CoV values, it can be observed that FRP effectiveness factor proposed by Chen & Teng combined with that for steel stirrups proposed in this paper provides the lowest scatter (0.20). Even if ACI effectiveness factor gives the best average value, it leads to the highest scatter (0.31), similar to that obtained by using Mofidi & Chaallal equations (0.29). As for effectiveness factor named as “first approach”, as well as those proposed by CNR and fib, scatter values range between 0.24 and 0.27. All that said, it can be stated that the procedure to calculate effectiveness factors which combines the best average accuracy (Avg value close to 1) and the highest reliability (low CoV value) is the one named “second approach”, which uses the equations proposed by Chen & Teng to evaluate effectiveness factor for FRP, and the equations proposed in section 4 to assess effectiveness factor for steel stirrups.

To provide an insight into the above-described differences, in Figure 3 are plotted the effectiveness factor values provided by the above-mentioned procedures for each specimens of the database. Moreover, power regression in the form $y = Ax^{-B}$, as well as coefficient of determination R^2, are given for each group of effectiveness factors in the case of U-shaped strengthening configuration. The results showed in Figure 3 help to explain the average and scatter values plotted in Figure 2. As a matter of fact, fib and Mofidi & Chaallal procedures, which averagely overestimates and underestimates the shear capacity of beams, respectively, are characterized by parameters A of power regression equal to 0.20 and 0.08, respectively.

Moreover, the high scatter in shear capacity assessment provided by ACI procedure is

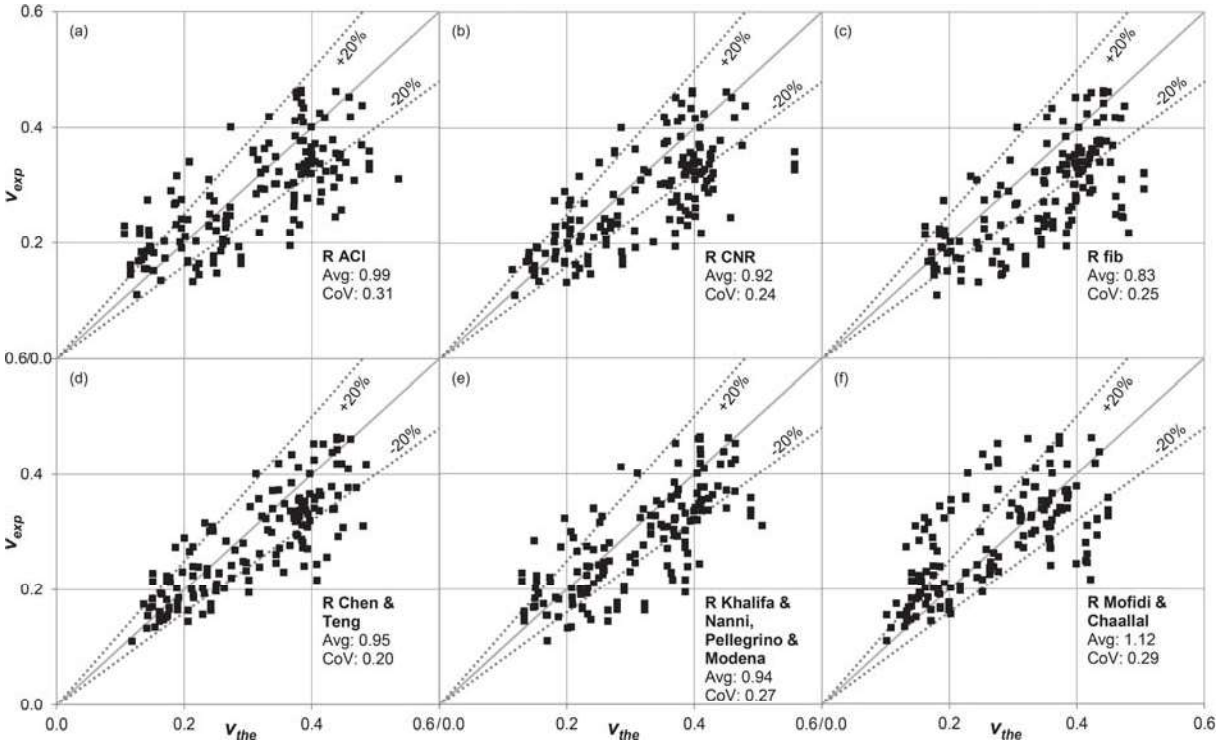

Figure 2: Experimental vs. theoretical shear capacity by using the proposed design-oriented model calculating effectiveness factors as suggested by: ACI (a); CNR (b); fib (c); Chen & Teng (second approach, sections 3.2 and 4) (d); Khalifa & Nanni, Pellegrino & Modena (first approach, sections 3.1 and 4) (e); Mofidi & Chaallal (f).

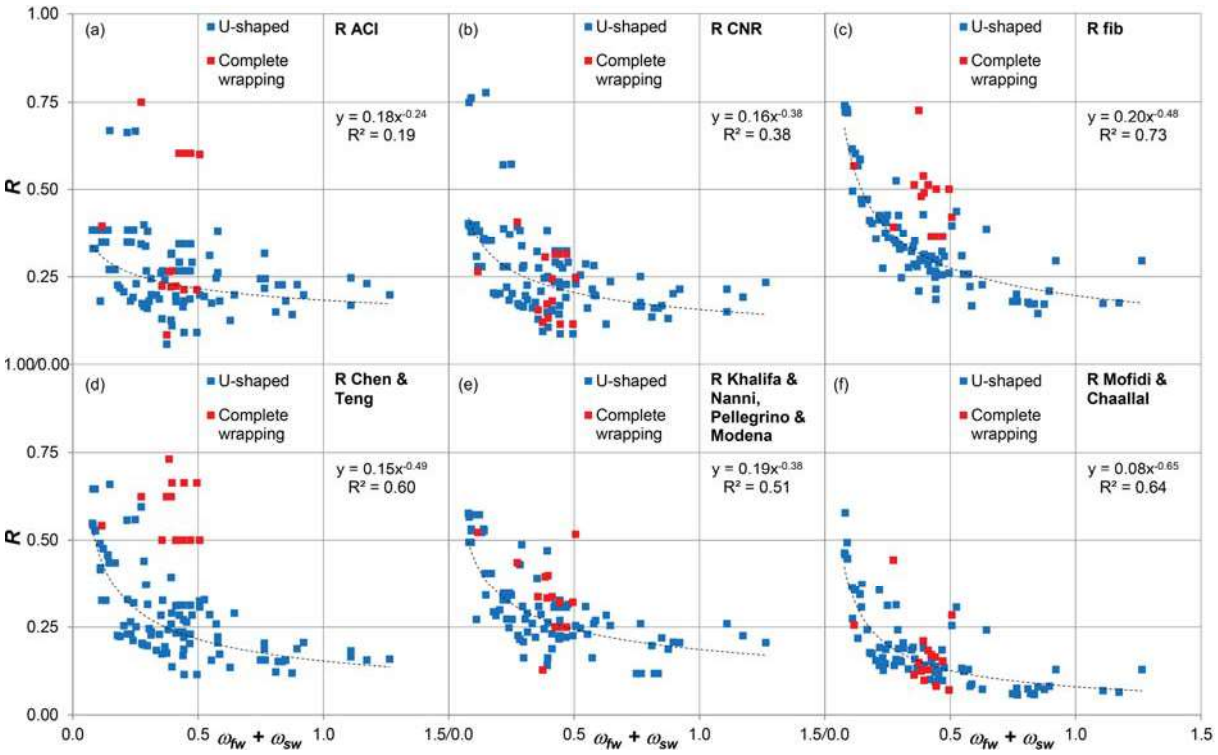

Figure 3: Effectiveness factors for FRP calculated as suggested by: ACI (a); CNR (b); fib (c); Chen & Teng (section 3.2) (d); Khalifa & Nanni, Pellegrino & Modena (section 3.1) (e); Mofidi & Chaallal (f).

confirmed by R^2 value, which is the lowest among those given by the analyzed procedures. With reference to complete wrapping configuration, it can be observed substantial differences

among the procedures. In fact, equations proposed by fib and Chen & Teng tend to provide R values higher than those given in the case of U-shaped configuration. On the contrary, equations proposed by CNR, Mofidi & Challal, and those listed in section 3.1, give R values similar to those for U-shaped strengthening scheme. With regard to ACI procedure, no trend can be noted, the R values being highly scattered.

Once the procedure to calculate effectiveness factors was selected, the proposed design-oriented model is validated against analytical results provided by code models suggested by ACI and CNR, as well as the proposed modified version of CNR, named CNRm.

In Figure 4 and Figure 5 are showed the results of the ratio between the experimental shear capacity and the theoretical prediction for each specimen belonging to the database and for each of the above-mentioned models, considering the two partial databases. Regarding results reported in Figure 4, all the models provide reliable results, even if some substantial difference can be observed. In fact, CNR model provides the best average value (1.00), to which correspond, however, the worst CoV value (0.24). With reference to the proposed model and ACI one, they provide similar values, characterized by low scatter and with a slight average overestimation of shear strength of beams. It is worth recalling that, in the case of FRP reinforcement and steel stirrups arranged with the same inclination, CNRm model gives the same results of the original CNR one.

Concerning beams having FRP reinforcement arranged with different inclination with respect to that of steel stirrups, the proposed model gives the best results. Although all the models overestimate in average shear capacity of beams, the proposed model gives the closest average to 1 and the lowest scatter. These results prove the accuracy and reliability of the proposed design-oriented model, and its superior performance in the case for which it was formulated, namely when FRP reinforcement and steel stirrups are oriented with different inclinations. It should be stressed that, in this latter case, the proposed model is the only one derived from a consistent physical model.

The results obtained in the two partial databases confirm that the use of an effectiveness factor that takes into account the strain experienced by FRP reinforcement oriented in any direction, leads to superior performance of the proposed model, which is thus able to account for the main interactions characterizing the shear resistance of a strengthened RC beam. On the contrary, model codes consider the brittle failure of FRP reinforcement, but neglect the interaction of the retrofitting system with both steel stirrups and concrete strut.

With regard to the results provided by CNR model and its modified version, CNRm, in Figure 5 it can be observed that the proposed calibration of ψ angle, which is the angle used in the evaluation of shear strength of concrete strut, slightly improves the performance of CNR model, reducing the scatter from 0.19 to 0.17. However, the proposed version of CNR model still significantly overestimates shear capacity beams, with an average value of 0.73.

To shed light on how the calibration of ψ angle influences the assessment of concrete strut inclination, in Figure 6 are illustrated $cot\theta$ values for specimens having FRP reinforcement and steel stirrups oriented with different inclinations. It can be noted that, for high amount of mechanical ratios of shear reinforcements, $cot\theta$ values are lower when ψ angle is computed by means of the simple procedure proposed. This contributes to reduce the overestimation of shear capacity affecting CNR model, increasing its reliability. It is worth noting that the proposed design-oriented model provides $cot\theta$ values which are equal to 2.5 in most of the analyzed cases. This is due to the different formulation used to calculate effectiveness factor for FRP, and to the presence of the effectiveness factor for steel stirrups, which reduces the denominator value of Eq. (6).

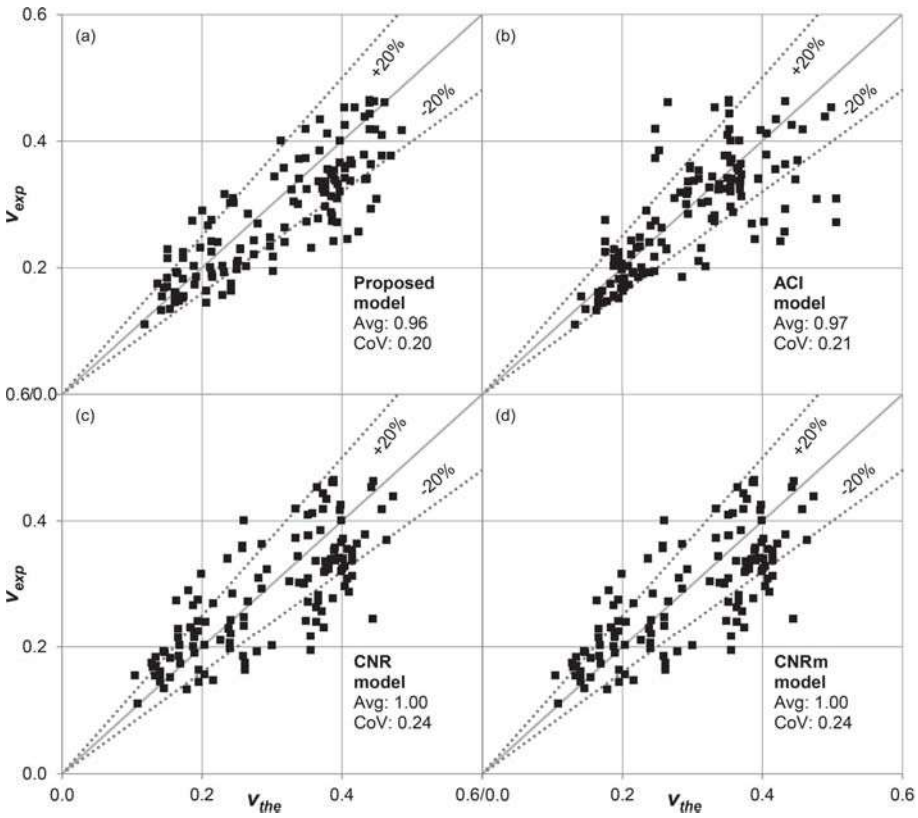

Figure 4: Experimental vs. theoretical shear capacity for DTB1: proposed design-oriented model with second approach (a); ACI (b); CNR (c); CNRm (d).

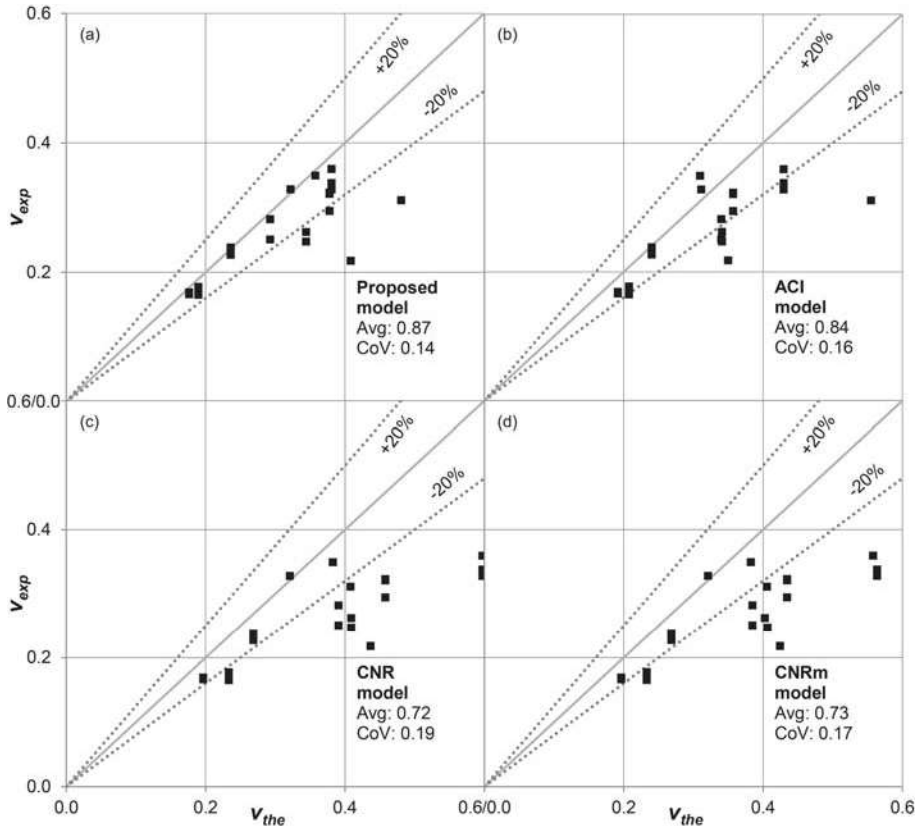

Figure 5: Experimental vs. theoretical shear capacity for DTB2: proposed design-oriented model with second approach (a); ACI (b); CNR (c); CNRm (d).

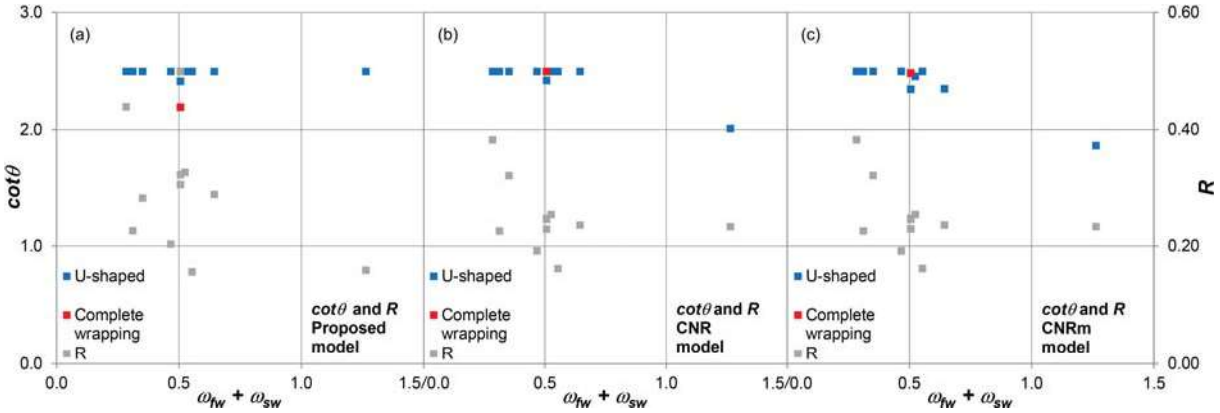

Figure 6: Inclination of concrete strut $cot\theta$ vs. sum of mechanical ratios of shear reinforcements $\omega_{fw} + \omega_{sw}$ for DTB2: proposed design-oriented model with second approach (a); CNR (b); CNRm (c).

8 PARAMETRIC ANALYSIS

Once the accuracy and reliability of the proposed design-oriented model were proved, in this section a parametric analysis is carried out, by varying inclination of FRP reinforcement, with the aim of evaluating its influence on shear capacity of retrofitted RC beams, calculated by means of the above-mentioned models based on variable inclination of concrete strut.

Among the several parameters influencing evaluation of shear capacity, mechanical ratios of shear reinforcements (ω_{fw} and ω_{sw}), as well as inclination of steel stirrups ($\alpha = 90°$), are assumed, while inclination of FRP reinforcement can vary in the range $45° \leq \beta \leq 90°$. To highlight some peculiar aspects of the proposed model, CNR one and its modified version CNRm, four different arrangements of shear reinforcement are assumed, considered representative of real applications: the first two, $\omega_{fw} = 0.15$; $\omega_{sw} = 0.05$ and $\omega_{fw} = 0.15$; $\omega_{sw} = 0.15$, are selected to compare the influence of the increment of steel shear reinforcement having low amount of FRP shear reinforcement; the other two, $\omega_{fw} = 0.20$; $\omega_{sw} = 0.40$ and $\omega_{fw} = 0.40$; $\omega_{sw} = 0.20$, are selected to compare shear strength in the case of high amount of steel/FRP shear reinforcement. In Figure 7 are showed curves of theoretical prediction of shear capacity obtained by means of the above models, calculated by varying angle of inclination of FRP reinforcement.

Generally speaking, the proposed model provides shear capacity values which are in most cases lower than those given by the two versions of CNR model, confirming the findings of Figure 5 against experimental results. Moreover, the proposed version of CNR model provides shear capacity values which are close to that of original CNR models for low amount of steel stirrups, while approach to those of the proposed design-oriented model when increasing amount of steel stirrups. With the exception of the case with very low amount of steel shear reinforcement (i.e. $\omega_{fw} = 0.15$; $\omega_{sw} = 0.05$), the difference between shear capacity values given by CNR and CNRm increases when angle of inclination of FRP approaches to 45°. As already stated above, this difference is due to the inability of CNR model to properly take into account the inclination of both steel stirrups and FRP reinforcement when assessing shear strength of concrete strut. This difference is magnified when contribution to shear capacity provided by steel stirrups is significant. More precisely, considering only the angle of inclination of FRP in evaluating shear capacity of concrete strut, CNR model provides shear capacity values of retrofitted beams closer to those of the other models when contribution given by FRP reinforcement prevails ($\omega_{fw} = 0.40$; $\omega_{sw} = 0.20$), while substantial differences can be noted when mechanical ratio of steel stirrups is considerably greater than that of FRP ($\omega_{fw} = 0.20$; $\omega_{sw} = 0.40$).

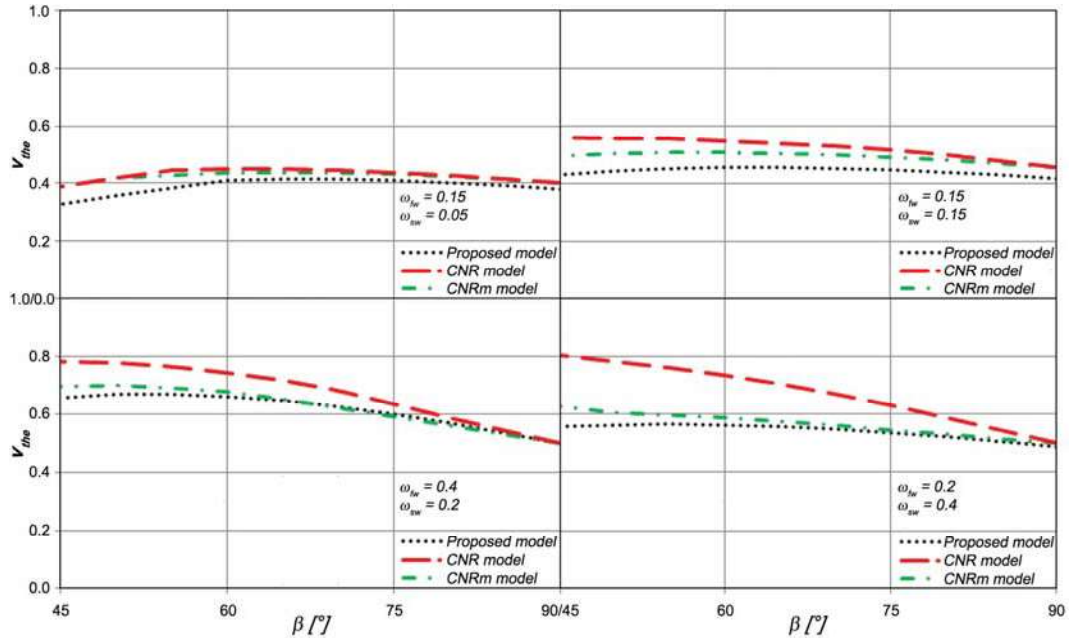

Figure 7: Shear capacity curves obtained with the proposed design-oriented model (black dotted line), CNR model (red dashed line), and CNRm model (green dash-dotted line), by varying angle of inclination of FRP reinforcement.

Focusing the attention on the variation of shear capacity by changing angle of inclination of FRP reinforcement, it can be observed that the optimal angle to obtain maximum shear strength varies on the basis of mechanical ratios of steel stirrups and FRP reinforcement assumed. For low amount of shear reinforcement, maximum shear strength is obtained for angle between 65° and 90°, while in the case of high amount of shear reinforcement, shear strength is maximized when FRP reinforcement is arranged with an angle less than 55°.

9 CONCLUSIONS

In the present paper was carried out a comparison between different procedures able to assess the effectiveness factors used to reduce shear contribution provided by FRP reinforcement when calculating shear capacity of retrofitted RC beams. In this regard, new procedures, by modification of already existing formulations, were proposed both for FRP reinforcement and steel stirrups. Concerning the latter, the proposed effectiveness factor aims to limit the strain of stirrups on the basis of the effective strain of FRP arranged in any direction. The above procedures were compared, together with those suggested by ACI, CNR, fib, and Mofidi and Chaallal [30], by calculating theoretical shear capacity of a group of 158 experimental tests, by using a proposed design-oriented model based on stress fields with variable inclination of concrete strut. This model has the advantage to simultaneously take into account the presence, and their mutual influence, of FRP reinforcement, steel stirrups, and concrete strut, when assessing the shear capacity, as well as the concrete stress field inclination. The model was formulated in order to accurately take into account FRP reinforcement and steel stirrups arranged with different inclinations in evaluating shear strength of concrete strut. In this latter case, other models based on truss mechanism, such as that proposed by CNR, fail to consider the presence of both FRP reinforcement and steel stirrups when evaluating shear capacity of concrete strut. For this reason, a new simple formulation developed for CNR model was proposed, aimed at obtaining an equivalent angle of inclination to be used in evaluation of shear capacity of concrete strut, weighted on the basis of shear contributions provided by FRP reinforcement and steel stirrups. To highlight the improvement given by the

proposed modification to CNR model, a parametric analysis was carried out, by varying inclination of FRP reinforcement, with the aim of evaluating its influence on shear capacity of retrofitted RC beams, calculated by means of the above-mentioned models based on variable inclination of concrete strut.

Once the effectiveness factors providing the best results were selected, the proposed model was compared against models proposed by ACI and CNR, as well as the proposed modified version of CNR, named CNRm. The main findings are summarized below:

- The procedure to calculate effectiveness factors which combines the best average accuracy (Avg value close to 1) and the highest reliability (low CoV value) is the one named "second approach", which uses the equations proposed by Chen & Teng to evaluate effectiveness factor for FRP, and the equations proposed in section 4 to assess effectiveness factor for steel stirrups.
- Concerning beams having FRP reinforcement arranged with different inclination with respect to that of steel stirrups, the proposed model gives the best results. Although all the models overestimate in average shear capacity of beams, the proposed model gives the closest average to 1 and the lowest scatter. These results prove the accuracy and reliability of the proposed design-oriented model, and its superior performance in the case for which it was formulated, namely when FRP reinforcement and steel stirrups are oriented with different inclinations.
- With regard to the results provided by CNR model and its modified version, CNRm, results showed that the proposed calibration of ψ angle, which is the angle used in the evaluation of shear strength of concrete strut, slightly improves the performance of CNR model. However, the proposed version of CNR model still significantly overestimates shear capacity of RC beams.
- Regarding the parametric analysis, the proposed version of CNR model provides shear capacity values which are close to those of original CNR models for low amount of steel stirrups, while approach to that of the proposed design-oriented model when increasing the amount of steel stirrups.
- Focusing the attention on the variation of shear capacity by changing angle of inclination of FRP reinforcement, it can be observed that the optimal angle to obtain maximum shear strength varies on the basis of mechanical ratios of steel stirrups and FRP reinforcement assumed. For low amount of shear reinforcement, maximum shear strength is obtained for angle between 65° and 90°, while in the case of high amount of shear reinforcement, shear strength is maximized when FRP reinforcement is arranged with an angle less than 55°.

10 APPENDIX

	Spec. no.	f_{cm} (MPa)	$b_w \times d$ (mm)	ρ_{sw} (%)	b_f (mm)	t_f (mm)	β (°)	ρ_{fw} (%)	f_{fu} (MPa)	E_f (GPa)	v_{exp} (-)
Sato et al. (1997) [51] a/d = 2.5 E_{sw} = 183 GPa f_{syw} = 387 MPa	No.2	35.7	150 × 240	0.42	C	0.11	90	0.15	3480	230	0.39
	No.3	35.3	150 × 240	0.42	C	0.11	90	0.15	3480	230	0.46
Deniaud & Cheng (2001) [38] a/d = 2.8	T6S4-C90	44.1	140 × 528	0.10	50	0.11	90	0.08	3400	230	0.19
	T6S4-G90	44.1	140 × 528	0.10	C	1.80	90	2.57	106	18	0.20

	Spec. no.	f_{cm} (MPa)	$b_w \times d$ (mm)	ρ_{sw} (%)	b_f (mm)	t_f (mm)	β (°)	ρ_{fw} (%)	f_{fu} (MPa)	E_f (GPa)	v_{exp} (-)
E_{sw} = 260 GPa f_{syw} = 520 MPa	T6S2-C90	44.1	140 × 528	0.20	50	0.11	90	0.08	3400	230	0.21
Deniaud & Cheng (2003) [39] a/d = 3.0 E_{sw} = 200 GPa f_{syw} = 520 MPa	T4S4-G90	30.0	140 × 362	0.10	50	1.80	90	2.57	106	18	0.30
	T4S2-G90	30.3	140 × 362	0.20	C	1.80	90	2.57	106	18	0.33
	T4S2-C45	29.4	140 × 362	0.20	C	0.70	45	0.50	442	45	0.33
	T4S2-Tri	30.4	140 × 362	0.20	C	2.10	60	3.00	124	8	0.35
Bousselham & Chaallal (2006) [35] a/d = 3.0 E_{sw} = 215 GPa f_{syw} = 650 MPa	SB-S1-0.5L	25.0	152 × 356	0.38	C	0.06	90	0.08	3100	243	0.46
	SB-S1-1L	25.0	152 × 356	0.38	C	0.11	90	0.14	3100	243	0.42
	SB-S1-2L	25.0	152 × 356	0.38	C	0.21	90	0.28	3100	243	0.44
Pellegrino & Modena (2006) [27] a/d = 3.0 E_{sw} = 210 GPa f_{syw} = 534 MPa	A-U1-C-17	41.4	150 × 250	0.39	C	0.17	90	0.22	3450	230	0.34
	A-U1-C-20	41.4	150 × 250	0.34	C	0.17	90	0.22	3450	230	0.32
	A-U1-S-17	41.4	150 × 250	0.39	C	0.17	90	0.22	3450	230	0.35
	A-U1-S-20	41.4	150 × 250	0.34	C	0.17	90	0.22	3450	230	0.34
	A-U2-C-17	41.4	150 × 250	0.39	C	0.33	90	0.44	3450	230	0.35
	A-U2-C-20	41.4	150 × 250	0.34	C	0.33	90	0.44	3450	230	0.33
	A-U2-S-17	41.4	150 × 250	0.39	C	0.33	90	0.44	3450	230	0.31
	A-U2-S-20	41.4	150 × 250	0.34	C	0.33	90	0.44	3450	230	0.30
Leung et al. (2007) [43] a/d = 2.9 (SB) a/d = 3.0 (MB) a/d = 2.7 (LB) E_{sw} = 210 GPa f_{syw} = 550 MPa	SB-U1	27.4	75 × 155	0.28	20	0.11	90	0.10	4200	235	0.45
	SB-F1	27.4	75 × 155	0.28	20	0.11	90	0.10	4200	235	0.46
	SB-F2	27.4	75 × 155	0.28	20	0.11	90	0.10	4200	235	0.46
	MB-U1	27.4	150 × 305	0.28	40	0.22	90	0.10	4200	235	0.27
	MB-U2	27.4	150 × 305	0.28	40	0.22	90	0.10	4200	235	0.28
	MB-F1	27.4	150 × 305	0.28	40	0.22	90	0.10	4200	235	0.42
	MB-F2	27.4	150 × 305	0.28	40	0.22	90	0.10	4200	235	0.44
	LB-U1	27.4	300 × 660	0.14	80	0.44	90	0.10	4200	235	0.23
	LB-U2	27.4	300 × 660	0.14	80	0.44	90	0.10	4200	235	0.23
	LB-F1	27.4	300 × 660	0.14	80	0.44	90	0.10	4200	235	0.36
	LB-F2	27.4	300 × 660	0.14	80	0.44	90	0.10	4200	235	0.36
Monti & Liotta (2007) [14] a/d = 3.5 E_{sw} = 210 GPa f_{syw} = 500 MPa	UF90	11.0	250 × 410	0.10	C	0.22	90	0.18	2600	390	0.25
	US60	11.0	250 × 410	0.10	150	0.22	60	0.08	2600	390	0.22
	US45+	11.0	250 × 410	0.10	150	0.22	45	0.06	2600	390	0.25
	US45++	11.0	250 × 410	0.10	50	0.22	45	0.06	2600	390	0.26
	UF45+ A	11.0	250 × 410	0.10	C	0.22	45	0.18	2600	390	0.33
	UF45++ B	11.0	250 × 410	0.10	C	0.22	45	0.18	2600	390	0.34
	UF45++ C	11.0	250 × 410	0.10	C	0.22	45	0.18	2600	390	0.36
	US45+ D	11.0	250 × 410	0.10	150	0.22	45	0.08	2600	390	0.32
	US45++ E	11.0	250 × 410	0.10	150	0.22	45	0.08	2600	390	0.32
	US45++ F	11.0	250 × 410	0.10	150	0.22	45	0.08	2600	390	0.29
	WS45+	11.0	250 × 410	0.10	50	0.22	45	0.06	2600	390	0.31
	USVA	10.6	250 × 410	0.10	150	0.22	38	0.05	2600	390	0.25
	USVA+	10.6	250 × 410	0.10	150	0.22	38	0.05	2600	390	0.28
Pellegrino & Modena (2008) [15] a/d = 3.0 E_{sw} = 210 GPa f_{syw} = 534 MPa	B-U1-C-14	46.2	150 × 240	0.48	C	0.17	90	0.22	3450	230	0.34
	B-U2-C-14	46.2	150 × 240	0.48	C	0.33	90	0.44	3450	230	0.35
	B-U1-C-17	46.2	150 × 240	0.39	C	0.17	90	0.22	3450	230	0.32
	B-U2-C-17	46.2	150 × 240	0.39	C	0.33	90	0.44	3450	230	0.33
Grande et al. (2009) [16] a/d = 3.4	RS4Wa	21.0	250 × 411	0.10	C	0.19	90	0.15	2600	392	0.26
	RS3Wa	21.0	250 × 411	0.13	C	0.19	90	0.15	2600	392	0.34
	RS2Wa	21.0	250 × 411	0.20	C	0.19	90	0.15	2600	392	0.31

	Spec. no.	f_{cm} (MPa)	$b_w \times d$ (mm)	ρ_{sw} (%)	b_f (mm)	t_f (mm)	β (°)	ρ_{fw} (%)	f_{fu} (MPa)	E_f (GPa)	v_{exp} (-)
E_{sw} = 210 GPa f_{syw} = 476 MPa	RS4Ub	21.0	250 × 411	0.10	C	0.19	90	0.15	2600	392	0.23
	RS3Ua	21.0	250 × 411	0.13	C	0.19	90	0.15	2600	392	0.28
	RS2Ua	21.0	250 × 411	0.20	C	0.19	90	0.15	2600	392	0.29
Belarbi et al. (2012) [34] a/d = 3.3 E_{sw} = 200 GPa f_{syw} = 276 MPa	8-NA	20.7	457 × 831	0.15	254	0.22	90	0.06	3792	228	0.24
	8-DMA	23.8	457 × 831	0.15	254	0.22	90	0.06	3792	228	0.23
	12-NA	28.9	457 × 831	0.10	254	0.22	90	0.06	3792	228	0.15
	12-DMA	30.5	457 × 831	0.10	254	0.22	90	0.06	3792	228	0.18
	12-PC	19.2	457 × 831	0.10	254	0.22	90	0.06	3792	228	0.29
	12-HS-PC	18.3	457 × 831	0.10	254	0.22	90	0.06	3792	228	0.27
Alzate et al. (2013) [32] a/d = 3.5 E_{sw} = 200 GPa f_{syw} = 500 MPa	U90S5-a(L)	37.0	250 × 420	0.11	300	0.29	90	0.14	4000	240	0.16
	U90S5-a(S)	37.0	250 × 420	0.11	300	0.29	90	0.14	4000	240	0.14
	U90S5-b(L)	28.0	250 × 420	0.11	300	0.29	90	0.14	4000	240	0.21
	U90S5-b(S)	28.0	250 × 420	0.11	300	0.29	90	0.14	4000	240	0.20
	U90C5-a(L)	24.5	250 × 420	0.11	C	0.29	90	0.23	4000	240	0.22
	U90C5-a(S)	24.5	250 × 420	0.11	C	0.29	90	0.23	4000	240	0.20
	U90C5-b(L)	22.6	250 × 420	0.11	C	0.29	90	0.23	4000	240	0.26
	U90C5-b(S)	22.6	250 × 420	0.11	C	0.29	90	0.23	4000	240	0.24
	U90S3-a(L)	20.5	250 × 420	0.11	300	0.17	90	0.08	3800	240	0.25
	U90S3-a(S)	20.5	250 × 420	0.11	300	0.17	90	0.08	3800	240	0.23
	U90S3-b(L)	22.6	250 × 420	0.11	300	0.17	90	0.08	3800	240	0.22
	U90S3-b(S)	22.6	250 × 420	0.11	300	0.17	90	0.08	3800	240	0.24
	U90S3-c(L)	28.0	250 × 420	0.11	300	0.17	90	0.08	3800	240	0.20
	U90S3-c(S)	28.0	250 × 420	0.11	300	0.17	90	0.08	3800	240	0.16
	U90C3-a(L)	30.2	250 × 420	0.11	C	0.17	90	0.13	3800	240	0.17
	U90C3-a(S)	30.2	250 × 420	0.11	C	0.17	90	0.13	3800	240	0.18
	U90C3-b(L)	30.2	250 × 420	0.11	C	0.17	90	0.13	3800	240	0.16
	U90C3-b(S)	30.2	250 × 420	0.11	C	0.17	90	0.13	3800	240	0.17
	U45S5(L)	30.7	250 × 420	0.11	300	0.29	45	0.14	4000	240	0.17
	U45S5(S)	30.7	250 × 420	0.11	300	0.29	45	0.14	4000	240	0.18
	U45S3-a(L)	20.5	250 × 420	0.11	300	0.17	45	0.08	3800	240	0.23
	U45S3-a(S)	20.5	250 × 420	0.11	300	0.17	45	0.08	3800	240	0.24
	U45S3-b(L)	30.7	250 × 420	0.11	300	0.17	45	0.08	3800	240	0.17
	U45S3-b(S)	30.7	250 × 420	0.11	300	0.17	45	0.08	3800	240	0.17
Panda et al. (2013) [49] a/d = 3.2 E_{sw} = 200 GPa f_{syw} = 252 MPa	S300-U-90	40.4	100 × 230	0.19	C	0.36	90	0.72	160	13	0.22
	S300-UA-90	40.4	100 × 230	0.19	C	0.36	90	0.72	160	13	0.23
	S200-U-90	42.1	100 × 230	0.28	C	0.36	90	0.72	160	13	0.22
	S200-UA-90	42.1	100 × 230	0.28	C	0.36	90	0.72	160	13	0.23
Baggio et al. (2014) [33] a/d = 2.9 E_{sw} = 200 GPa f_{syw} = 384 MPa	6-G-N	50.1	150 × 310	0.21	100	0.51	90	0.34	575	26	0.16
	7-PD-G-N	50.1	150 × 310	0.21	100	0.51	90	0.34	575	26	0.15
	8-PD-G-CA	50.1	150 × 310	0.21	100	0.51	90	0.34	575	26	0.15
	9-PD-G-GA	50.1	150 × 310	0.21	100	0.51	90	0.34	575	26	0.16
Colalillo & Sheikh (2014) [37] a/d = 3.1 E_{sw} = 195 GPa f_{syw} = 501 MPa	S5-US	47.6	400 × 545	0.07	100	1.00	90	0.25	961	95	0.11
	S5-UA	47.6	400 × 545	0.07	C	1.00	90	0.50	961	95	0.13
	S5-CS	47.6	400 × 545	0.07	100	1.00	90	0.25	961	95	0.16
	S2-US	47.5	400 × 545	0.14	100	1.00	90	0.25	961	95	0.13
	S2-UA	47.5	400 × 545	0.14	C	1.00	90	0.50	961	95	0.15
Ozden et al. (2014) [48] a/d = 3.8 E_{sw} = 200 GPa f_{syw} = 249 MPa	FBwo-C	12.4	120 × 339	0.14	20	0.13	90	0.05	4300	238	0.27
	FBw-C	12.4	120 × 339	0.14	20	0.13	90	0.05	4300	238	0.36
	PBw-C	12.4	120 × 339	0.14	20	0.13	90	0.05	4300	238	0.29
	FBwo-G	12.4	120 × 339	0.14	20	0.16	90	0.06	3400	73	0.27
	FBw-G	12.4	120 × 339	0.14	20	0.16	90	0.06	3400	73	0.34
	PBw-G	12.4	120 × 339	0.14	20	0.16	90	0.06	3400	73	0.34

	Spec. no.	f_{cm} (MPa)	$b_w \times d$ (mm)	ρ_{sw} (%)	b_f (mm)	t_f (mm)	β (°)	ρ_{fw} (%)	f_{fu} (MPa)	E_f (GPa)	v_{exp} (-)
	FBwo-Hi-C	12.4	120 × 339	0.14	20	0.14	90	0.05	2600	640	0.24
	FBw-Hi-C	12.4	120 × 339	0.14	20	0.14	90	0.05	2600	640	0.27
	PBw-Hi-C	12.4	120 × 339	0.14	20	0.14	90	0.05	2600	640	0.31
Mofidi & Chaallal (2014) [44] a/d = 3.0 E_{sw} = 206 GPa f_{syw} = 540 MPa	WT-ST-50	31.0	152 × 350	0.38	88	0.11	90	0.07	3450	230	0.33
	WT-ST-70	31.0	152 × 350	0.38	88	0.11	90	0.10	3450	230	0.34
	WT-SH-100	31.0	152 × 350	0.38	C	0.11	90	0.14	3450	230	0.34
Mofidi et al. (2014) [45] a/d = 3.0 E_{sw} = 205 GPa f_{syw} = 650 MPa	S1-LS-NE	33.7	152 × 350	0.38	40	2.00	90	0.60	1350	90	0.34
	S1-LS-PE	33.7	152 × 350	0.38	40	2.00	90	0.60	1350	90	0.37
	S1-EB-NA	33.7	152 × 350	0.38	C	0.11	90	0.14	3450	230	0.36
El-Saikaly et al. (2014) [40] a/d = 3.0 E_{sw} = 200 GPa f_{syw} = 580 MPa	S1-EB	28.0	152 × 350	0.25	C	0.38	90	0.50	894	65	0.32
	S1-LS	28.0	152 × 350	0.25	20	1.40	90	0.21	2250	120	0.30
	S1-LS-Rope	28.0	152 × 350	0.25	20	1.40	90	0.21	2250	120	0.38
	S3-EB	28.0	152 × 350	0.38	C	0.38	90	0.50	894	65	0.38
	S3-LS	28.0	152 × 350	0.38	20	1.40	90	0.21	2250	120	0.36
	S3-LS-Rope	28.0	152 × 350	0.38	20	1.40	90	0.21	2250	120	0.42
Qin et al. (2015) [50] a/d = 3.1 E_{sw} = 210 GPa f_{syw} = 542 MPa	S00	29.6	125 × 295	0.29	C	1.00	90	1.60	986	96	0.37
Chen et al. (2016) [36] a/d = 3.0 E_{sw} = 200 GPa f_{syw} = 416 MPa	S8-U	46.1	200 × 320	0.25	50	0.17	90	0.08	4361	226	0.23
	S8-UFA1	46.1	200 × 320	0.25	50	0.17	90	0.08	4361	226	0.24
	S8-UFA2	46.1	200 × 320	0.25	50	0.17	90	0.08	4361	226	0.28
Frederick et al. (2017) [42] a/d = 3.2 E_{sw} = 200 GPa f_{syw} = 415 MPa	TB2	27.2	130 × 235	0.17	C	0.15	90	0.23	1400	119	0.37
	TB4	27.2	130 × 235	0.17	C	0.15	90	0.23	1400	119	0.42
El-Saikaly et al. (2017) [41] a/d = 3.0 E_{sw} = 200 GPa f_{syw} = 580 MPa	EBS-NA	28.0	152 × 350	0.25	C	0.38	90	0.50	894	65	0.32
	EBL-NA	28.0	152 × 350	0.25	20	2.00	90	0.30	1350	90	0.30
	EBS-BL	28.0	152 × 350	0.25	C	0.38	90	0.50	894	65	0.37
	EBS-ER	28.0	152 × 350	0.25	C	0.38	90	0.50	894	65	0.40
	EBL-RF	28.0	152 × 350	0.25	20	2.00	90	0.30	1350	90	0.41
	EBL-RW	28.0	152 × 350	0.25	20	2.00	90	0.30	1350	90	0.38
Nguyen-Minh et al. (2018) [46] a/d = 2.3 E_{sw} = 205 GPa f_{syw} = 342 MPa	A1-2.3-C	30.6	120 × 406	0.16	75	1.00	90	0.83	986	96	0.41
	A1-2.3-G	30.6	120 × 406	0.16	75	1.30	90	1.08	575	26	0.40
	A1-2.3-G-C.	30.6	120 × 406	0.16	C	1.30	90	2.17	575	26	0.43
	A1-2.3-C-C.	30.6	120 × 406	0.16	C	1.00	90	1.67	986	96	0.45
	A2-2.3-C	30.6	120 × 406	0.16	75	2.00	90	1.67	986	96	0.43
	B1-2.3-C	44.4	120 × 406	0.16	75	1.00	90	0.83	986	96	0.32
	B1-2.3-G	44.4	120 × 406	0.16	75	1.30	90	1.08	575	26	0.32
	B1-2.3-G-C.	44.4	120 × 406	0.16	C	1.30	90	2.17	575	26	0.34
	B1-2.3-C-C.	44.4	120 × 406	0.16	C	1.00	90	1.67	986	96	0.36
	B2-2.3-C	44.4	120 × 406	0.16	75	2.00	90	1.67	986	96	0.34
	C1-2.3-C	58.7	120 × 406	0.16	75	1.00	90	0.83	986	96	0.29
	C1-2.3-G	58.7	120 × 406	0.16	75	1.30	90	1.08	575	26	0.27
	C1-2.3-G-C.	58.7	120 × 406	0.16	C	1.30	90	2.17	575	26	0.31
	C1-2.3-C-C.	58.7	120 × 406	0.16	C	1.00	90	1.67	986	96	0.32
	C2-2.3-C	58.7	120 × 406	0.16	75	2.00	90	1.67	986	96	0.30

	Spec. no.	f_{cm} (MPa)	$b_w \times d$ (mm)	ρ_{sw} (%)	b_f (mm)	t_f (mm)	β (°)	ρ_{fw} (%)	f_{fu} (MPa)	E_f (GPa)	v_{exp} (-)
	M1-a	42.8	200 × 493	0.12	50	0.17	90	0.04	2739	263	0.18
	M1-b	42.8	200 × 493	0.12	50	0.17	90	0.04	2739	263	0.17
	M1A	39.0	200 × 493	0.12	50	0.17	90	0.04	2739	263	0.19
	M1B	38.5	200 × 493	0.12	50	0.17	90	0.04	2739	263	0.19
Oller et al.	M2A	39.0	200 × 493	0.12	100	0.17	90	0.07	2739	263	0.20
(2019) [47]	M2B	38.5	200 × 493	0.12	100	0.17	90	0.07	2739	263	0.19
a/d = 3.0	H1-a	44.4	200 × 493	0.12	50	0.17	90	0.04	2739	263	0.17
E_{sw} = 200 GPa	H2-a	44.4	200 × 493	0.12	100	0.17	90	0.07	2739	263	0.17
f_{syw} = 646 MPa	H2-b	49.7	200 × 493	0.12	100	0.17	90	0.07	2739	263	0.15
	H2A	44.7	200 × 493	0.12	100	0.17	90	0.07	2739	263	0.20
	H2B	49.6	200 × 493	0.12	100	0.17	90	0.07	2739	263	0.18
	H3A	44.7	200 × 493	0.12	C	0.17	90	0.17	2739	263	0.19
	H3B	49.6	200 × 493	0.12	C	0.17	90	0.17	2739	263	0.19

Table 1: Characteristics of specimens and experimental results

REFERENCES

[1] E. Elettore, F. Freddi, M. Latour, G. Rizzano, Design and analysis of a seismic resilient steel moment resisting frame equipped with damage-free self-centering column bases. *Journal of Constructional Steel Research*, **179**, 106543, 2021. https://doi.org/10.1016/10.1016/j.jcsr.2021.106543.

[2] S. Ramhormozian, G.C. Clifton, M. Latour, G.A. Macrae, Proposed simplified approach for the seismic analysis of multi-storey moment resisting framed buildings incorporating friction sliders. *Buildings*, **9** (5), 130, 2019. https://doi.org/10.3390/buildings9050130.

[3] P. Colajanni, L. La Mendola, A. Monaco, S. Pagnotta, Design of RC joints equipped with hybrid trussed beams and friction dampers. *Engineering Structures*, **227**, 111442, 2021. https://doi.org/10.1016/j.engstruct.2020.111442.

[4] P. Colajanni, L. La Mendola, A. Monaco, S. Pagnotta, Dissipative connections of rc frames with prefabricated steel-trussed-concrete beams. *Ingegneria Sismica* **37** (1), 51-63, 2020. http://ingegneriasismica.org/product/5-2020-1-dissipative-connections-of-rc-frames-with-prefabricated-steel-trussed-concrete-beams/

[5] S. Pagnotta, P. Colajanni, L. La Mendola, A. Monaco, Seismic response of RC frames with HSTC beams endowed with friction damper devices. *18th Conference of the Italian National Association of Earthquake Engineering (ANIDIS 2019)*, Ascoli Piceno, Italy, September 15-19, 2019. https://doi.org/10.1400/271271.

[6] P. Colajanni, L. La Mendola, A. Monaco, S. Pagnotta, Design of friction connections in R.C. structures with hybrid steel-trussed-concrete beams. *18th Conference of the Italian National Association of Earthquake Engineering (ANIDIS 2019)*, Ascoli Piceno, Italy, September 15-19, 2019. https://doi.org/10.1400/271300.

[7] P. Colajanni, F. De Domenico, A. Recupero, N. Spinella, Concrete columns confined with fibre reinforced cementitious mortars: experimentation and modeling. *Construction and Building Materials*, **52**, 375-384, 2014. https://doi.org/10.1016/j.conbuildmat.2013.11.048.

[8] G. Campione, F. Cannella, M.F. Ferrotto, M. Gianquinto, Compressive behavior of FRP externally wrapped R.C. column with buckling effects of longitudinal bars. *Engineering Structures*, **168**, 809-818, 2018. https://doi.org/10.1016/j.engstruct.2018.05.027.

[9] N. Spinella, P. Colajanni, A. Recupero, F. Tondolo, Ultimate shear of RC beams with corroded stirrups and strengthened with FRP. *Buildings*, **9** (2), 34, 2019. https://doi.org/10.3390/buildings9020034.

[10] P. Colajanni, A. Recupero, N. Spinella, Shear Strength Degradation Due to Flexural Ductility Demand in Circular R.C. Columns. *Bulletin of Earthquake Engineering*, **13** (6), 1795–1807, 2015. https://doi.org/10.1007/s10518-014-9691-0.

[11] G. Campione, M.F. Ferrotto, M. Papia, Flexural response of RC beams failing in shear. *Practice Periodical on Structural Design and Construction*, **25** (4), 4020028. https://doi.org/10.1061/(ASCE)SC.1943-5576.0000507.

[12] ACI (American Concrete Institute). 2017. Guide for the Design and Construction of Externally Bonded FRP Systems for Strengthening Concrete Structures. ACI 440.2R-17. Farmington Hills, MI: ACI.

[13] CAN/CSA (Canadian Standards Association). 2006. *Canadian highway bridge design code*. S6-06. Mississagua, Canada: CAN/CSA.

[14] G. Monti, M. Liotta, Tests and design equations for FRP strengthening in shear. *Construction and Building Materials*, **21** (4), 799–809, 2007. https://doi.org/10.1016/j.conbuildmat.2006.06.023.

[15] C. Pellegrino, C. Modena, An experimentally based analytical model for the shear capacity of FRP-strengthened reinforced concrete beams. *Mechanics of Composite Materials*, **44** (3), 231-244, 2008. https://doi.org/10.1007/s11029-008-9016-y.

[16] E. Grande, M. Imbimbo, A. Rasulo, Effect of transverse steel on the response of RC beams strengthened in shear by FRP: experimental study. *Journal of Composites for Construction*, **13** (5), 405-414, 2009. https://doi.org/10.1061/(ASCE)1090-0268(2009)13:5(405).

[17] CNR (Consiglio Nazionale delle Ricerche – National Research Council). 2013. Istruzioni per la Progettazione, l'Esecuzione ed il Controllo di Interventi di Consolidamento Statico mediante l'utilizzo di Compositi Fibrorinforzati. CNR-DT-200/R1. Rome, Italy: CNR. [In Italian].

[18] DAfStB (Deutscher Ausschuss für Stahlbeton - German Committee for Structural Concrete). 2012. Strengthening of Concrete Members with Adhesively Bonded Reinforcement. Beuth-Verlag, Berlin, Germany. [Original in German, English version].

[19] A. Darby, J. Clarke, J.D. Shave, T. Ibell, 2012. "Design guidance for strengthening concrete structures using fibre composite materials: report of a Concrete Society Working Party." Technical Report Vol. 55, 3rd ed. The Concrete Society.

[20] Fib (Fédération internationale du béton - *International Federation* for Structural Concrete). 2019. *Externally applied FRP reinforcement for concrete structures*. Fib bulletin 90. Lausanne, Switzerland: Fib.

[21] CEN (European Committee for Standardization). 2004. *Design of concrete structures, part 1.1: general rules and rules for buildings*. EN1992-1-1. Brussels, Belgium: CEN.

[22] P. Colajanni, S. Pagnotta, A. Recupero, N. Spinella, Shear resistance analytical evaluation for RC beams with transverse reinforcement with two different inclinations. *Materials and Structures*, **53** (1), 18, 2020. https://doi.org/10.1617/s11527-020-1452-8.

[23] P. Colajanni, L. La Mendola, A. Recupero, N. Spinella, Stress field model for strengthening of shear-flexure critical RC beams. *Journal of Composites for Construction*, **21** (5), 04017039, 2017. https://doi.org/10.1061/(ASCE)CC.1943-5614.0000821.

[24] P. Colajanni, L. La Mendola, G. Mancini, A. Recupero, N. Spinella, Shear capacity in concrete beams reinforced by stirrups with two different inclinations. *Engineering Structures*, **81**, 444-453, 2014. https://doi.org/10.1016/j.engstruct.2014.10.011.

[25] J.F. Chen, J.G. Teng, Shear capacity of FRP-strengthened RC beams: FRP debonding. *Construction and Building Materials*, **17** (1), 27-41, 2003. https://doi.org/10.1016/S0950-0618(02)00091-0.

[26] J.F. Chen, J.G. Teng, Shear capacity of fiber-reinforced polymer-strengthened reinforced concrete beams: fiber reinforced polymer rupture. *Journal of Structural Engineering*, **129** (5), 615-625, 2003. https://doi.org/10.1061/(ASCE)0733-9445(2003)129:5(615).

[27] C. Pellegrino, C. Modena, Fiber-reinforced polymer shear strengthening of reinforced concrete beams: experimental study and analytical modeling. *ACI Structural Journal*, **103** (5), 720-728, 2006. https://doi.org/10.14359/16924.

[28] A. Khalifa, A. Nanni, Improving shear capacity of existing RC T-section beams using CFRP composites. *Cement and Concrete Composites*, **22** (3), 165-174, 2000. https://doi.org/10.1016/S0958-9465(99)00051-7.

[29] A. Khalifa, A. Nanni, Rehabilitation of rectangular simply supported RC beams with shear deficiencies using CFRP composites. *Construction and Building Materials*, **16** (3), 135-146, 2002. https://doi.org/10.1016/S0950-0618(02)00002-8.

[30] A. Mofidi, O. Chaallal, Shear strengthening of RC beams with EB FRP: Influencing factors and conceptual debonding model. *Journal of Composites for Construction*, **15** (1), 62-74, 2011. https://doi.org/10.1061/(ASCE)CC.1943-5614.0000153.

[31] N. Spinella, Modeling of shear behavior of reinforced concrete beams strengthened with FRP. *Composite Structures*, **215**, 351-364, 2019. https://doi.org/10.1016/j.compstruct.2019.02.073.

[32] A. Alzate, A. Arteaga, A. De Diego, D. Cisneros, R. Perera, Shear strengthening of reinforced concrete members with CFRP sheets. *Materiales de Construcción*, **63** (310), 251-265, 2013. https://doi.org/10.3989/mc.2012.06611.

[33] D. Baggio, K. Soudki, M. Noël, Strengthening of shear critical RC beams with various FRP systems. *Construction and Building Materials*, **66**, 634-644, 2014. https://doi.org/10.1016/j.conbuildmat.2014.05.097.

[34] A. Belarbi, S.W. Bae, A. Brancaccio, Behavior of full-scale RC T-beams strengthened in shear with externally bonded FRP sheets. *Construction and Building Materials*, **32**, (10), 27-40, 2012. https://doi.org/10.1016/j.conbuildmat.2010.11.102.

[35] A. Bousselham, O. Chaallal, Behavior of reinforced concrete T-beams strengthened in shear with carbon fiber-reinforced polymer - an experimental study. *ACI Structural Journal*, **103** (3), 339-347, 2006. https://doi.org/10.14359/15311.

[36] G.M. Chen, Z. Zhang, Y.L. Li, X.Q. Li, C.Y. Zhou, T-section RC beams shear-strengthened with anchored CFRP U-strips. *Composite Structures*, **144**, 57-79, 2016. https://doi.org/10.1016/j.compstruct.2016.02.033.

[37] M.A. Colalillo, S.A. Sheikh, Behavior of shear-critical RC beams strengthened with FRP - experimentation. *ACI Structural Journal*, **111** (6), 1373-1384, 2014. https://doi.org/10.14359/51687035.

[38] C. Deniaud, J.J.R. Cheng, Shear behavior of reinforced concrete T-Beams with externally bonded fiber-reinforced polymer sheets. *ACI Structural Journal*, **98** (3): 386-394, 2001. https://doi.org/10.14359/10227.

[39] C. Deniaud, J.J.R. Cheng, Reinforced concrete T-beams strengthened in shear with fiber reinforced polymer sheets. *Journal of Composites for Construction* **7** (4), 302-310, 2003. https://doi.org/10.1061/(ASCE)1090-0268(2003)7:4(302).

[40] G. El-Saikaly, A. Godat, O. Chaallal, New anchorage technique for FRP shear-strengthened RC T-beams using CFRP rope. *Journal of Composites for Construction*, **19** (4), 04014064, 2014. https://doi.org/10.1061/(ASCE)CC.1943-5614.0000530.

[41] G. El-Saikaly, O. Chaallal, B. Benmokrane.. "Comparison of anchorage systems for RC T-beams strengthened in shear with EB-CFRP." *6th Asia-Pacific Conference on FRP in Structures (APFIS2017)*, Singapore, 1-5, 2017.

[42] F.F.R. Frederick, U.K. Sharma, V.K. Gupta, Influence of end anchorage on shear strengthening of reinforced concrete beams using CFRP composites, *Current Science*, **112** (5), 973-981, 2017. https://doi.org/10.18520/cs/v112/i05/973-981.

[43] C.K.Y. Leung, Z. Chen, S. Lee, M. Ng, M. Xu, J. Tang, Effect of size on the failure of geometrically similar concrete beams strengthened in shear with FRP strips, *Journal of Composites for Construction*, **11** (5), 487-496, 2007. https://doi.org/10.1061/(ASCE)1090-0268(2007)11:5(487).

[44] A. Mofidi, O. Chaallal, Tests and design provisions for reinforced-concrete beams strengthened in shear using FRP sheets and strips. International Journal *of* Concrete *Structures and Materials*, **8**, 117–128, 2014. https://doi.org/10.1007/s40069-013-0060-1.

[45] A. Mofidi, S. Thivierge, O. Chaallal, Y. Shao, Behavior of reinforced concrete beams strengthened in shear using L-shaped CFRP plates: experimental investigation. *Journal of Composites for* Construction, **18** (2): 04013033, 2014. https://doi.org/10.1061/(ASCE)CC.1943-5614.0000398.

[46] L. Nguyen-Minh, D. Vo-Le, D. Tran-Thanh, T.M. Pham, C. Ho-Huu, M. Rovňák, Shear capacity of unbonded post-tensioned concrete T-beams strengthened with CFRP and GFRP U-wraps. *Composite Structures*, **184**, 1011-1029, 2018. https://doi.org/10.1016/j.compstruct.2017.10.072.

[47] E. Oller, M. Pujol, A. Marí, Contribution of externally bonded FRP shear reinforcement to the shear strength of RC beams. *Composites Part B:* Engineering, **164**, 235-248, 2019. https://doi.org/10.1016/j.compositesb.2018.11.065.

[48] S. Ozden, H.M. Atalay, E. Akpinar, H. Erdogan, Y.Z. Vulaş, Shear strengthening of reinforced concrete T-beams with fully or partially bonded fibre-reinforced polymer composites. *Structural Concrete*, **15** (2), 229–239, 2014. https://doi.org/10.1002/suco.201300031.

COMPDYN 2021

Proceedings of the
8th International Conference on
Computational Methods in Structural Dynamics and Earthquake Engineering

M. Papadrakakis, M. Fragiadakis (Eds.)

First Edition, September 2021

ISBN (set): 978-618-85072-5-8
ISBN (vol I): 978-618-85072-3-4

Institute of Structural Analysis and Antiseismic Research
National Technical University of Athens, Greece